OPTIMAL LAYOUT OF LONG-SPAN TRUSS-GRIDS—II

YEP KONG MIN, ROMAN SANDLER and GEORGE I. N. ROZVANY
Department of Civil Engineering, Monash University, Clayton, Victoria, Australia

Abstract—In Part I of this study, a general theory of optimal layout for long-span truss-grids was outlined, and then it was applied to circular simply supported truss-grids whose span length does not exceed a certain limiting value. The optimal solution for the above problem was shown to consist of a purely circumferential moment field. It is established in Part II that for simply supported circular truss-grids of longer spans, the optimal solution takes on a more complicated topography consisting of both circumferential and radial moment fields. In addition, optimal solutions are presented for circular truss-grids that are built-in (clamped) along their edge. Finally, a weight comparison for various types of solutions is given.

OPTIMAL SOLUTION FOR LONG-SPAN SIMPLY SUPPORTED CIRCULAR TRUSS-GRIDS

It was established in Part I that for simply supported circular truss-grids within a limiting radius [see eqn (45) and Fig. 6 of Part I], the optimal solution consists of purely circumferential moments ($M_\theta \geq 0$, $M_r = 0$, chords in circumferential direction only). For greater radii ($R > R_{\lim}$), the same type of solution would violate one of the optimality conditions [eqn (37)† or (44) corresponding to $M_r = 0$] and, hence, it cannot be optimal.

It will be shown herein that for truss-grids with $R > R_{\lim}$ the optimal solution consists of the following:

(i) a purely circumferential moment field ($M_\theta \geq 0$, $M_r \equiv 0$) in an inner region ($r \leq a$);

(ii) a purely radial moment field ($M_\theta \equiv 0$, $M_r \leq 0$) in the outer region;

(iii) a circumferential positive moment impulse along the circular edge of the truss-grid. The mechanical function of the latter is to balance the radial moments along the simply supported edge by a (concentrated) ring of heavy circumferential chords.

Denoting the displacements $u_1(r)$ and $u_2(r)$ for the inner and outer region of the above type of solution, the optimality conditions (36)–(39), boundary condition

$$u_2'(R) = -(1 + c)R, \tag{53}$$

and continuity condition [$u_1(a) = u_2(a)$] furnishes the following displacement fields:

for $r \leq a$:

$$u_1' = -(1 + u_1)(r + cR), \tag{54a}$$

$$u_1(r) = e^{\{a^2 + cR[a + R(1 + c)] - (r + cR)^2\}/2}\{\cosh[(R - a)\beta]$$
$$+ [(1 + c/2)R/\beta] \sinh[(R - a)\beta]\} - 1; \tag{54b}$$

for $r \geq a$:

$$-u_2'' = -(1 + u_2) + cRu_2', \tag{55a}$$

$$u_2(r) = e^{\alpha(R - r)}\{\cosh[(R - r)\beta] + [(R + \alpha)/\beta] \sinh[(R - r)\beta]\} - 1, \tag{55b}$$

---

† Equation numbers (1)–(52) refer to Part I of this study.

where

$$\alpha = cR/2, \qquad \beta = (1 + \alpha^2)^{1/2}. \tag{56}$$

The boundary condition given in eqn (53) follows from (38) since at $r = R$ the inequality $M_\theta > 0$ holds (M_θ takes on a positive impulse).

For the solution in eqns (54) and (55), the additional continuity condition $u'_1(a) = u'_2(a)$ furnishes the optimal value of a:

$$\tanh[(R - a)\beta] = (R - a)\beta/(aR + \alpha R + \alpha a - 1). \tag{57}$$

Optimal a values (a_{opt}), given by eqn (57) for various shear cost factor (c) and radius (R) values, are shown in Fig. 1, and the corresponding displacements are shown in Fig. 2. It can be checked easily that for $R \leq R_{lim}$ [eqn (45) and Fig. 6 of Part I], $a_{opt} = R$, which means that the optimal solutions consist of an inner region (with $M_\theta \geq 0$, $M_r \equiv 0$) only. This agreement with the R_{lim} value derived in Part I constitutes an independent check on the range of validity of the two types of optimal solutions.

It is shown in the Appendix that the displacements $u_2(r)$ in the outer region also satisfy the optimality condition (39) for $M_\theta \equiv 0$.

The moment field in the *inner region* ($r \leq a$, $M_\theta \geq 0$, $M_r \equiv 0$) is given again by eqn (47). For the outer region ($r \geq a$, $M_\theta \equiv 0$, $M_r \leq 0$), the equilibrium condition

$$(rM_r)'' = -r + rM_r + cR(rM_r)' \tag{58}$$

and boundary conditions

$$(rM_r)' \big|_{r=a} = -M_\theta, \qquad M_r(a) = 0, \tag{59}$$

furnish the moment field:

$$\text{(for } r \geq a) \quad rM_r = e^{\alpha r}[A \cosh(r\beta) + B \sinh(r\beta)] - cR + r \quad \text{(for } r \geq a) \tag{60}$$
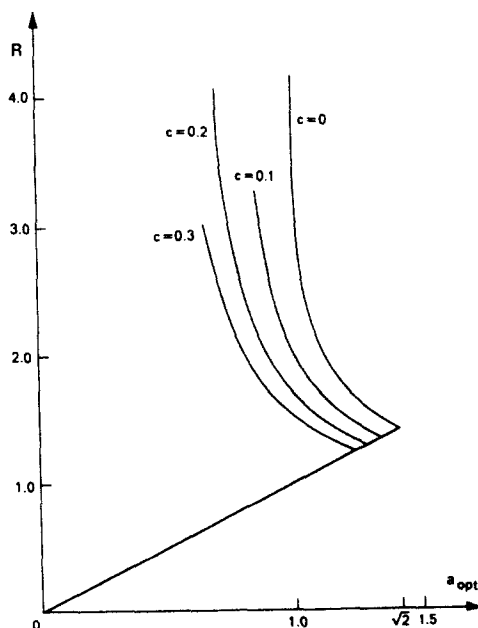

Fig. 1. Simply supported circular trusses: optimal radius of region boundary as a function of the radius of support (R) and shear cost factor (c).
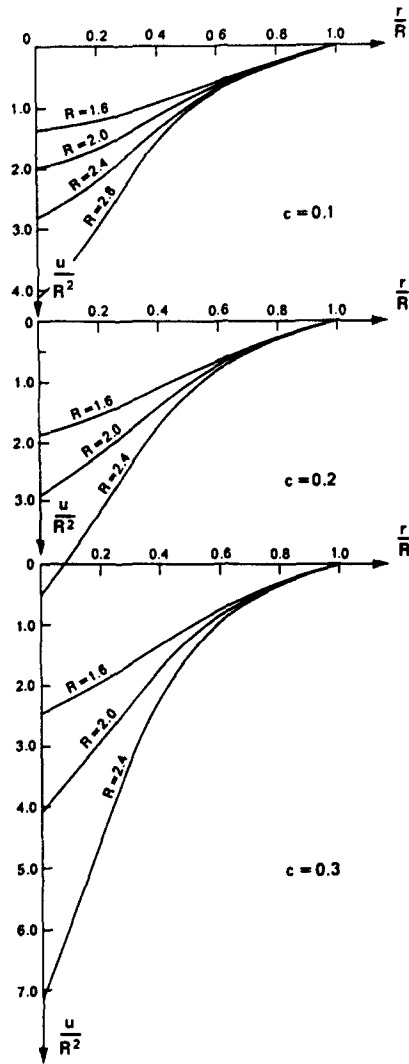
Fig. 2. Pragerian deflection fields for truss-grids with $R > R_{lim}$.

with

$$A = -\sinh[a\beta]\left\{e^{a(\alpha+a/2)}\left[e^{2\alpha^2}\sqrt{\pi/2}\,2\alpha\left(\text{erf}\frac{a+cR}{\sqrt{2}} - \text{erf}\frac{cR}{\sqrt{2}}\right) - 1\right]\right/\beta$$

$$+ (cR - a)\,e^{-\alpha a}\{\cosh(a\beta) + [\alpha\sinh(a\beta)]/\beta\right\} \tag{61}$$

$$B = \cosh(a\beta)\left\{\sqrt{\pi/2}\,2\alpha\,e^{(a^2/2)+2\alpha^2+\alpha a}\left(\text{erf}\frac{a+cR}{\sqrt{2}} - \text{erf}\frac{cR}{\sqrt{2}}\right) - e^{a^2/2+\alpha a}\right.$$

$$- (cR - a)\,e^{-\alpha a}[\beta\tanh(a\beta) + \alpha]\right\}\right/\beta. \tag{62}$$

The optimal moment fields for $R = 1.8$ and various c values are shown in Fig. 3. The vertical dimension of the M_θ-impulse indicates its integrated value $RM_r(R)$. The actual magnitude of the impulse (Dirac distribution, δ), following from equilibrium is

$$M_{\theta EDGE} = RM_r(R)\delta(R - r), \tag{63}$$

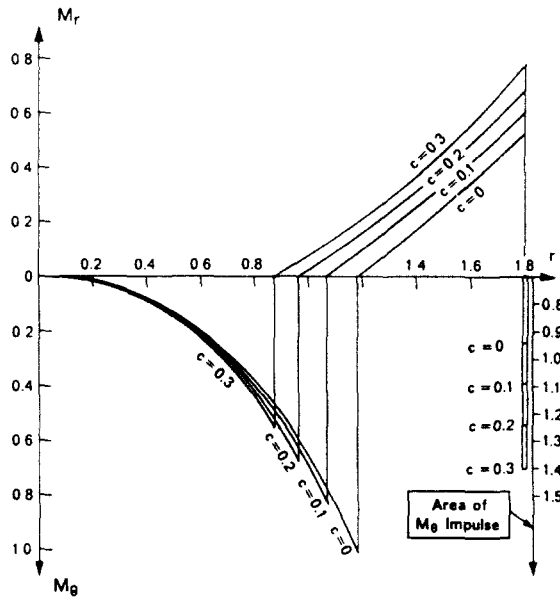where $RM_r(R)$ can be readily determined from eqns (60)–(62).

Fig. 3. Optimal moment fields for truss-grids with $R > R_{\lim}$.

The total weight Φ of the system can be obtained by evaluating $\Phi = 2 \int_0^R \psi r \, dr$, taking the impulse at $r = R$ into consideration or by taking the total shear $V = (rM_r)'$ at $r = R$, less the external load (R^2) plus the total weight $[-2R^2 M_r(R)]$ caused by the moment impulse:

$$\Phi_{\min} = 2[(rM_r)' \mid_{r=R} - R^2 M_r(R)] - R^2, \tag{64}$$

which can be evaluated by making use of eqns (60)–(62).

Alternatively, the minimum total weight can be determined from eqn (4), making use of (54)–(56):

$$\Phi = 2 \int_0^R ur \, dr = 2 \int_0^a u_1 r \, dr + 2 \int_a^R u_2 r \, dr. \tag{65}$$

The first integration in the right-hand side of (65) can be carried out directly, and the second one after expressing u_2 from (55a):

$$u_2 = u_2'' - 1 + cRu_2'. \tag{66}$$

The resulting total weight becomes

$$\Phi_{\min} = 2\{\cosh[(R - a)\beta] + (R + \alpha) \sinh[(R$$

$$- a)\beta]/\beta\} \, e^{(a^2/2 + \alpha R + \alpha a)} \left[-e^{-(2\alpha a + a^2/2)} \right.$$

$$+ 1 - 2\alpha \, e^{2\alpha^2} \sqrt{\pi/2} \left(\operatorname{erf} \frac{cR + a}{\sqrt{2}} - \operatorname{erf} \frac{cR}{\sqrt{2}} \right) \right] \tag{67}$$

$$+ 2\{Ru_2'(R) - au_2'(a) + u_2(a) + cR[-au_2(a)$$

$$- u_2'(R) + u_2'(a) + cRu_2(a) + R - a]\} - R^2.$$

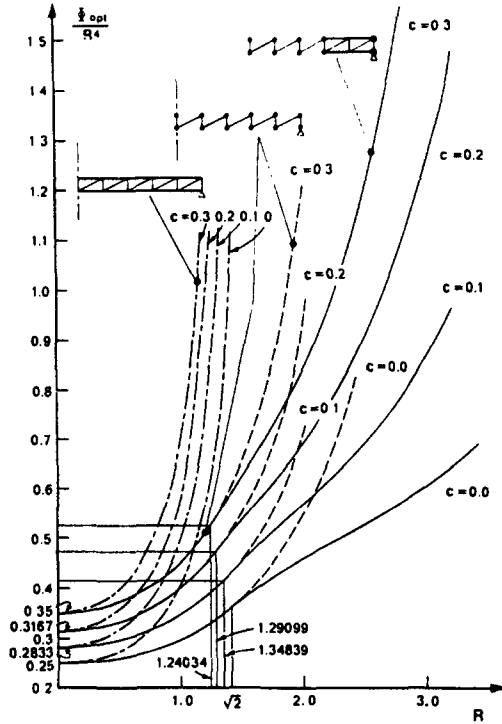The results from eqns (67) and (64) have shown a complete numerical agreement.

Fig. 4. Total structural weight for various types of layouts (optimal solution in continuous line).

Figure 4 shows the total structural weight Φ for various types of solutions as a function of R and c. Optimal solutions are represented in continuous line. It can be seen that at the limiting radius R_{lim}, the purely circumferential solution ($M_\theta \geqslant 0$, $M_r \equiv 0$) and the partly circumferential, partly radial solution have the same total weight. However, for $R > R_{lim}$, the purely circumferential solution (broken line) becomes highly
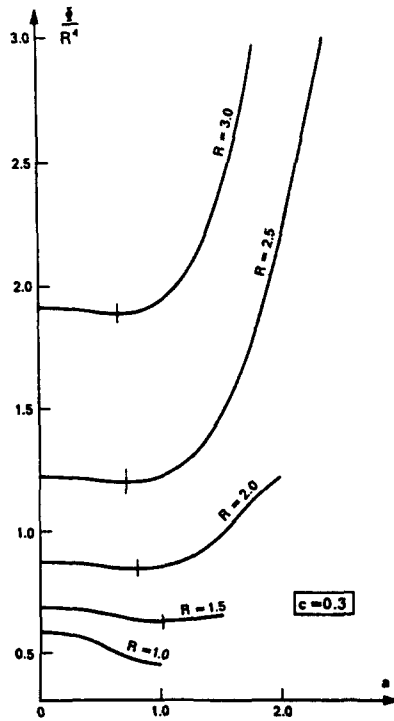

Fig. 5. Total structural weight as a function of region boundary radius for solutions with a purely circumferential moment field in the inner region and a purely radial moment field in the outer region.

uneconomical. The information in Fig. 4 constitutes a second independent confirmation of the values of the limiting radius in Fig. 6 of Part 1, originally derived from the optimality criterion (37).

Figure 5 indicates graphically the variation of the total weight Φ, given by eqn (67) or (64) with eqns (60)–(62), as a function of the region boundary radius a for the case of $c = 0.3$. It can be seen that the cost curves have a single local minimum, and the latter occurs at the a_{opt} values (vertical line segments in Fig. 5) given in Fig. 1. Figure 5 therefore constitutes an independent confirmation of the results derived from optimality criteria. It can also be seen from Fig. 5 that for $R \le R_{lim}$ (e.g. $R = 1$), $a_{opt} = R$.

Figure 4 also shows in dash-dot line the total weight of a third (nonoptimal) solution consisting of purely radial moments ($M_r \ge 0$, $M_\theta \equiv 0$) which is derived in the next section.

A COMPARISON OF OPTIMAL AND NONOPTIMAL SOLUTIONS: A PURELY RADIAL MOMENT FIELD

In order to demonstrate the extent of savings achieved by layout optimization, a nonoptimal solution with $M_r \ge 0$, $M_\theta \equiv 0$, will be considered. The equilibrium equation then becomes

$$(rM_r)'' = -r - rM_r + cR(rM_r)', \tag{68}$$

and the boundary conditions

$$(rM_r)' \big|_{r=0} = 0, \qquad M_r(R) = 0, \tag{69}$$

furnishing

$$rM_r = e^{\alpha r}\{[e^{-\alpha R}\lambda R(c + 1) - \sin(\lambda R)] \cos(\lambda r) + [\cos(\lambda R) - \alpha e^{-\alpha R}R(c$$
$$+ 1)] \sin(\lambda r)\}/[\lambda \cos(\lambda R) - \alpha \sin(\lambda R)] - cR - r, \tag{70}$$

where

$$\alpha = cR/2, \qquad \lambda = (1 - \alpha^2)^{1/2}. \tag{71}$$

The total cost can again be calculated by either integrating the specific cost $\psi = M_r - cR(rM_r)'/r$,

$$\Phi = 2 \int_0^R \psi r \, dr = 2 \int_0^R [M_r r - cR(rM_r)'] \, dr, \tag{72}$$

or by taking the total shear force $V = (rM_r)'/r$ along the edge ($r = R$) and subtracting the total external load (in nondimensional notation: R^2):

$$\Phi = -2(rM_r)' \big|_{r=R} - R^2. \tag{73}$$

The result in eqn (73) can also be obtained by expressing ψ from the equilibrium equation (33) and then integrating the expression $\int_0^R \psi r \, dr$ by parts. Both eqns (72) and (73) furnish the total structural weight

$$\Phi = (-2)\{[e^{\alpha R}\lambda - R(1 + c) \sin(\lambda R)]/[\lambda \cos(\lambda R) - \alpha \sin(\lambda R)] - 1\} - R^2. \tag{74}$$

The same total structural weight may be derived from eqn (4) furnishing $\Phi =$

$2 \int_0^R ur \, dr$ where u must satisfy eqn (36) for $M > 0$:

$$-u'' = 1 + u + cRu' \tag{75}$$

together with the boundary conditions

$$u'(0) = -[1 + u(0)]cR, \qquad u(R) = 0. \tag{76}$$

The above dual formulation is valid because for the considered solution $u(r)$ is still a Pragerian deflection for a structural universe consisting of *radial trusses only*.

Equations (75) and (76) imply

$$u = e^{-\alpha r}[A \cos(\lambda r) + B \sin(\lambda r)] - 1, \tag{77}$$

with

$$\begin{aligned}
A &= \lambda \, e^{\alpha R}/[\lambda \cos(\lambda R) - \alpha \sin(\lambda R)], \\
B &= \alpha \, e^{\alpha R}/[\alpha \sin(\lambda R) - \lambda \cos(\lambda R)],
\end{aligned} \tag{78}$$

giving

$$u = e^{\alpha(R-r)}[\lambda \cos(\lambda r) - \alpha \sin(\lambda r)]/[\lambda \cos(\lambda R) - \alpha \sin(\lambda R)] - 1. \tag{79}$$

The total weight can then be determined by integrating by parts and expressing repeatedly u from eqn (75):

$$\begin{aligned}
\Phi/2 &= \int_0^R ur \, dr = [(-u' - r - cRu)r]_0^R - \int_0^R (-u' - r - cRu) \, dr \\
&= (-u'(R) - R)R + R^2/2 - u(0) + cR[-u'(R) - R + u'(0) + cRu(0)] \quad (80)
\end{aligned}$$

Expressing $u'(0)$ from eqn (76), we have after simplifications

$$\Phi/2 = -R(1 + c)u'(R) - R^2(c + c^2 + 1/2) - u(0). \tag{81}$$

Substituting

$$\begin{aligned}
u(0) &= \lambda\theta \, e^{\alpha R} - 1, \\
u'(R) &= \theta[-2\alpha\lambda \cos(\lambda R) + (\alpha^2 - \lambda^2) \sin(\lambda R)]
\end{aligned}$$

with

$$\theta = [\lambda \cos(\lambda R) - \alpha \sin(\lambda R)]^{-1}, \tag{82}$$

we have

$$\begin{aligned}
\Phi = -2\{(R + cR)\theta[-2\alpha\lambda \cos(\lambda R) &+ (\alpha^2 - \lambda^2) \sin(\lambda R)] \\
&+ \lambda\theta \, e^{\alpha R} - 1 + R^2(c + c^2 + 1/2)\}, \quad (83)
\end{aligned}$$

or

$$\begin{aligned}
\Phi &= -2\theta\{-(R + cR)2\alpha\lambda \cos(\lambda R) + (R + cR)(\alpha^2 - \lambda^2) \sin(\lambda R) \\
&\quad + \lambda \, e^{\alpha R} + [cR^2 + c^2R^2][\lambda \cos(\lambda R) - \alpha \sin(\lambda R)]\} + 2 - R^2 \\
&= -2\theta\{\lambda \, e^{\alpha R} + \sin(\lambda R)[(R + 2\alpha)(-\alpha^2 - \lambda^2)]\} + 2 - R^2 \quad (84)
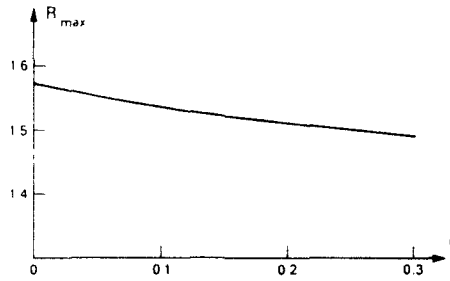\end{aligned}$$

Fig. 6. Spanning capacity (R_{max}) for purely radial moment fields.

Observing that $-\alpha^2 - \lambda^2 = -\alpha^2 - 1 + \alpha^2 = -1$, eqn (84) then reduces to eqn (74).

Figure 4 shows the variation of the total weight Φ of the purely radial solution with R and c in dash-dot line. It can be seen that for $R \to 0$ (no self-weight), both radial and circumferential solutions give the same total structural weight Φ.

The purely radial solution reaches its spanning capacity ($\Phi \to \infty$) when in eqn (74)

$$\lambda \cos(\lambda R) - \alpha \sin(\lambda R) = 0. \tag{85}$$

The variation of the spanning capacity R_{max} as a function of the shear cost factor c is shown in Fig. 6.

CIRCULAR TRUSS-GRIDS WITH BUILT-IN EDGES

Considering circular truss-grids with built-in (clamped) edges, the optimal solution will be shown to be similar to that for long-span simply supported circular grids, except that the kinematic boundary condition at the edge becomes

$$u_2'(R) = -cR, \tag{86}$$

and no M_θ-impulse is necessary to balance the radial moments at the edge. The boundary condition in eqn (86) can be derived by considering the cost functional in (35) with $rV = M_\theta - (rM_r)'$ and applying the usual transversality conditions (e.g. [1], p. 22) for variations of M_r at $r = R$. Alternatively, the modified Prager–Shield condition, (3) and (19), requires a shear strain of

$$\xi = -u_2'(R) = cR[1 + u(R)] = cR \tag{87}$$

at the clamped end ($r = R$). For eqn (86) and the remaining boundary conditions $u_2(R) = 0$, and continuity condition $u_1(a) = u_2(a)$, the optimality conditions (36) and (38) furnish the Pragerian displacements:

for $0 \leqslant r \leqslant a$:

$$M_r \equiv 0, \qquad M_\theta \geqslant 0, \qquad -u_1' = (1 + u_1)(r + cR),$$

$$u_1(r) = \{\cosh[(R - a)\beta] + (\alpha/\beta) \sinh[(R - a)\beta]\}$$

$$\times e^{-\{(r^2 - a^2)/2 + cR[r - (R + a)/2]\}} - 1; \tag{88}$$

for $a \leqslant r \leqslant R$:

$$M_\theta \equiv 0, \qquad M_r \leqslant 0, \qquad -u_2'' = -(1 + u_2) + cRu_2', \tag{89}$$

$$u_2 = (e^{\alpha(R - r)}/\beta)\{\beta \cosh[(R - r)\beta] + \alpha \sinh[(R - r)\beta]\} - 1.$$

Table 1. Comparison of total structural weight (ϕ) of various designs and percentage (p) of excess weight of nonoptimal designs over the optimal solution considering the case $c = 0.3$.

	Design		
	A	B	C
R	Optimal solution	$M_r \equiv 0, M_\theta > 0$ throughout	$M_\theta \equiv 0, M_r > 0$ throughout
1.5	0.628239	0.653255	$> \infty$
		(3.98%)	
2.5	1.199229	3.109522	$> \infty$
		(159.3%)	
3.0	1.889007	12.352402	$> \infty$
		(553.9%)	

The optimal value of a is then furnished by the kinematic condition $u_1'(a) = u_2'(a)$, implying

$$(a + \alpha)/\beta = \{\beta \sinh[(R - a)\beta] + \alpha \cosh[(R - a)\beta]\}/\{\beta \cosh[(R - a)\beta] + \alpha \sinh[(R - a)\beta]\}. \quad (90)$$

The variation of a_{opt} as a function of c and R is shown in Fig. 7. For the special case of $c = 0$, eqn (90) reduces to

$$a = \tanh(R - a), \quad (91)$$

which was derived earlier by Rozvany and Wang[2]

The total cost $\Phi = 2 \int_0^R ur \, dr$ is given by the same expression as in eqn (67) except that the coefficient $(R + \alpha)$ of the sinh term is replaced by α.

The moment field with $M_\theta \geq 0$, $M_r \equiv 0$ in the inner region is again given by (47) and in the outer region with $M_r \leq 0$, $M_\theta \equiv 0$ by eqn (62). The total structural weight Φ, given by the total shear force along the edge less the nondimensional external load,
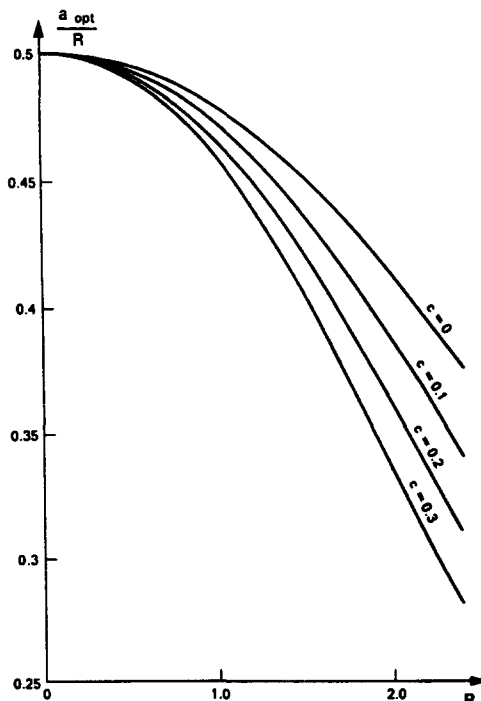

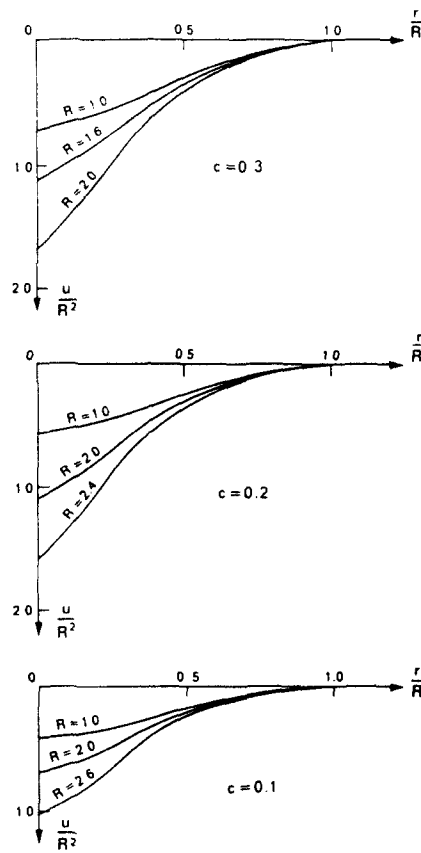Fig. 7. Clamped circular: truss-grids optimal values of the region boundary.

Fig. 8. Pragerian deflection fields for clamped circular truss-grids.

is furnished by

$$\Phi = -2(rM_r)' \big|_{r=R} - R^2 \tag{92}$$

and has been found in complete agreement numerically with the total weight given by the modified version of eqn (67).

The displacement fields given by eqns (88) and (89) are shown in Fig. 8, and the corresponding moment fields are shown in Fig. 9.
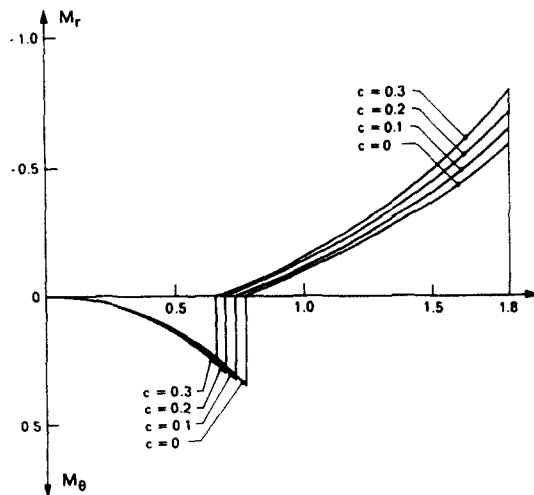

Fig. 9. Optimal moment fields for clamped circular truss-grids.

EXTENT OF SAVINGS ACHIEVED BY LAYOUT OPTIMIZATION

In this section, the total structural weight of the following three types of designs are compared for simply supported circular truss-grids:

(A) *Optimal solution* with $M_\theta \geq 0$, $M_r \equiv 0$ in the inner region and $M_\theta \equiv 0$, $M_r \leq 0$ in the outer region with an M_θ-impulse along the edge.

(B) *Purely circumferential solution* with $M_\theta \geq 0$, $M_r \equiv 0$.

(C) *Purely radial solution* with $M_r \geq 0$, $M_\theta \equiv 0$.

Considering truss-grids with purely moment-dependent cost functions ($c = 0$), it was noted earlier[2] that a design C is highly uneconomical for longer spans. For example, at $R = \sqrt{2}$, the total weight of design C was found 1317% higher than that of design B, see [2].

In the case of the more realistic cost functions with a nonzero c-value, the savings achieved by the optimal solution become even higher. In Table 1, we compare the total structural weight for the particular cases of $R = 1.5, 2.5$ and 3, and $c = 0.3$. It can be seen from Fig. 6 that for $c = 0.3$, the maximum nondimensional radius is 1.49, at which the structural weight would reach theoretically an infinite value. Beyond this maximum radius (spanning capacity), the structure is not even capable of carrying its own weight. This conclusion is implied by the symbols "$> \infty$" in Table 1.

Actual values of the nondimensional structural weight 2Φ for designs A and B are also shown in Table 1, together with the percentage of the excess weight of design B over design A:

$$p = (\Phi_B - \Phi_A)/\Phi_A. \tag{100}$$

It will be seen that at $R = 3$, $c = 0.3$, even the weight difference between designs A and B is most significant.

CONCLUSIONS

(1) The problem of optimizing the layout of long-span truss-grids was examined. Noting that at such spans self-weight (dead load) becomes the governing load component, a general theory and optimality criteria were presented for determining the optimal layout of vertical trusses over a horizontal area of any shape and for any load condition. In estimating the weight-per-unit length of the truss, it was assumed that the weight of the chords is governed by bending moment and the weight of the web members by the shear force on the truss.

(2) The above theory was then applied to axially symmetric truss-grids. In such systems, chords resisting *moments* may run in radial or circumferential directions, whereas the web members transmitting *shear* are contained in planes in the radial direction. Then optimization consists of finding the proportions of loads carried by radial and circumferential moments (chords). However, the solutions obtained satisfy the *sufficient* conditions of optimality of the general theory (for not necessarily axisymmetric systems) and hence it is established that for axisymmetric loads and supports, the optimal design is in fact axially symmetric.

(3) Considering *simply supported circular truss-grids*, it has been found that for shorter spans a purely circumferential moment field is optimal. At longer spans, the optimal solution consists of purely circumferential (positive) moments in an inner region, purely radial (negative) moments in an outer region and a circumferential moment-impulse (concentrated chord-rings) along the edge. At very short spans, the self-weight can be neglected and then *any* statically admissible combination of positive radial and circumferential moments is equally optimal.

(4) For circular truss-grids with a built-in edge (full fixity along the perimeter), the optimal solution always consists of a purely circumferential moment field in the inner region and a purely radial moment field in the outer region.

(5) In all optimal solutions having two regions, the radius (a) of the optimal region boundary decreases with the radius (R) of the truss-grid (Figs. 1 and 7).

(6) It can be seen from Fig. 4 that layout optimization of long-span truss-grids usually results in considerable savings in structural weight amounting to several hundred percent excess weight of the nonoptimal solution over the optimal one.

(7) All solutions in this paper were obtained in a closed analytical form. Moreover, the same optimal solution was obtained from both primal and dual formulation. This study demonstrates the potential value of continuum formulation and relatively sophisticated mathematical methods in problems of practical significance.

REFERENCES

1. G. I. N. Rozvany, *Optimal Design of Flexural Systems*. In English. Pergamon Press, Oxford (1976): *ibid.* In Russian. Stroiijdat, Moscow (1980).
2. G. I. N. Rozvany and C.-M. Wang, Optimal layout theory: allowance for self-weight. *J. Eng. Mech. Div. ASCE* 110(EM2), 66–83 (1984).

APPENDIX

PROOF THAT THE PRAGERIAN DISPLACEMENT FIELD IN THE OUTER REGION SATISFIES THE OPTIMALITY CONDITION FOR ZERO CIRCUMFERENTIAL MOMENTS

The considered displacement field is given in eqn (55b), and the optimality condition for $M_\theta = 0$ is in eqn (39). By eqn (55b),

$$u_2' = -e^{\alpha(R-r)}\{(2\alpha + R)\cosh[\beta(R - r)] + [\alpha(R + \alpha)/\beta + \beta]\sinh[\beta(R - r)]\}. \tag{A1}$$

Then one of the inequality conditions under (39),

$$-u_2' \leq (1 + u_2)(r + cR), \tag{A2}$$

implies

$$\text{(for } a < r < R) \quad (2\alpha + R)\cosh[\beta(R - r)] + [(\alpha R + 1 + 2\alpha^2)/\beta]\sinh[\beta(R - r)]$$
$$\leq (r + 2\alpha)\{\cosh[\beta(R - r)] + [(R + \alpha)/\beta]\sinh[\beta(R - r)]\}. \tag{A3}$$

or

$$(R - r)\cosh[\beta(R - r)] \leq [rR + \alpha R - 1 + r\alpha)/\beta]\sinh[\beta(R - r)]. \tag{A4}$$

or

$$\text{(for } a < r < R) \quad \tanh[\beta(R - r)] \leq [2\beta(R - r)]/[r(R + \alpha) + \alpha R - 1]. \tag{A5}$$

Moreover, for $r \leq a$ and $r = R$, $M_\theta > 0$ and hence by (38) the inequalities (A2)–(A5) are satisfied as equalities: for $r = a$ and $r = R$,

$$\tanh[\beta(R - r)] = [2\beta(R - r)]/[r(R + \alpha)] + \alpha R - 1]. \tag{A6}$$

For $\beta > 1$ and $r < R$ implies a known property of the function tanh( ):

$$\frac{d^2}{dr^2}\{\tanh[\beta(R - r)]\} < 0. \tag{A7}$$

Moreover, let

$$f(r) = K(R - r)/(r - b), \tag{A8}$$

with $b < r < R$.

Then the inequality $d^2 f/dr^2 > 0$ holds for any positive constants K, R and b. This can be shown by taking

$$(1/K)f(r) = \frac{R - r}{r - b} + \frac{r - b}{r - b} - 1 = \frac{R - b}{r - b} - 1, \quad (1/K)\frac{d^2 f}{dr^2} = 2\frac{R - b}{(r - b)^3} > 0. \tag{A9}$$

The RHS of eqn (A5) can be brought to the form in (A8) by the following rearrangement:

$$f(r) = \frac{2\beta(R - r)}{r(R + \alpha) + \alpha R - 1} = \frac{1}{R + \alpha} \frac{2\beta(R - r)}{r - [(1 - \alpha R)/(R + \alpha)]} .$$ (A10)

Since $a < r < R$ in the considered region, it is only necessary to show that

$$a > (1 - \alpha R)/(R + \alpha).$$ (A11)

This can be shown on the basis of eqn (A6) with $r = a$. Since in the latter the left-hand side and the numerator of the right-hand side are positive, the denominator of the right-hand side must also be positive;

$$a(R + \alpha) + \alpha R - 1 > 0,$$ (A12)

which implies (A11). Finally, since $\tanh[\beta(R - r)] = f(r)$ at $r = a$ and $r = R$, $\tanh[\beta(R - r)]$ is concave and $f(r)$ is convex for $a \leqslant r \leqslant R$, eqn (A5), and hence (A2), is now proved. It can be shown similarly that for $a \leqslant r \leqslant R$,

$$(1 + u_2)(-r + cR) \leqslant u_2'.$$ (A13)